NAVAL POSTGRADUATE SCHOOL

MONTEREY, CALIFORNIA

THESIS

PERFORMANCE ANALYSIS OF AN ALTERNATIVE TO TRELLIS CODED MODULATION FOR WAVEFORMS TRANSMITTED OVER A CHANNEL WITH PULSE-NOISE INTERFERENCE

by

Mario Rui Monteiro Marques

June 2008

Thesis Advisor:	Clark Robertson
Second Reader:	Tri Ha

THIS PAGE INTENTIONALLY LEFT BLANK

REPORT DOCUMENTATION PAGE			*Form Approved OMB No. 0704-0188*
Public reporting burden for this collection of information is estimated to average 1 hour per response, including the time for reviewing instruction, searching existing data sources, gathering and maintaining the data needed, and completing and reviewing the collection of information. Send comments regarding this burden estimate or any other aspect of this collection of information, including suggestions for reducing this burden, to Washington headquarters Services, Directorate for Information Operations and Reports, 1215 Jefferson Davis Highway, Suite 1204, Arlington, VA 22202-4302, and to the Office of Management and Budget, Paperwork Reduction Project (0704-0188) Washington DC 20503.			
1. AGENCY USE ONLY (*Leave blank*)	**2. REPORT DATE** June 2008	**3. REPORT TYPE AND DATES COVERED** Master's Thesis	
4. TITLE AND SUBTITLE: Performance Analysis of an Alternative to Trellis Coded Modulation for Waveforms Transmitted over a Channel with Pulse-Noise Interference			**5. FUNDING NUMBERS**
6. AUTHOR(S) Mario Rui Monteiro Marques			
7. PERFORMING ORGANIZATION NAME(S) AND ADDRESS(ES) Naval Postgraduate School Monterey, CA 93943-5000			**8. PERFORMING ORGANIZATION REPORT NUMBER**
9. SPONSORING /MONITORING AGENCY NAME(S) AND ADDRESS(ES) N/A			**10. SPONSORING/MONITORING AGENCY REPORT NUMBER**
11. SUPPLEMENTARY NOTES The views expressed in this thesis are those of the author and do not reflect the official policy or position of the Department of Defense or the U.S. Government.			
12a. DISTRIBUTION / AVAILABILITY STATEMENT Approved for public release; distribution is unlimited			**12b. DISTRIBUTION CODE**
13. ABSTRACT (maximum 200 words) The performance of a communication system having almost the same spectral efficiency as a trellis coded modulation (TCM) system with $r = 2/3$ convolutional encoding and 8-*ary* phase-shift keying (8-PSK) modulation is investigated. TCM is a common solution to the problem of adding forward error correction (FEC) coding without an attendant increase in channel bandwidth. The primary drawback to TCM is that the achievable coding gain is limited by the maximum practical number of states in the convolutional encoder. The alternative system considered uses (63, 37) Reed-Solomon (RS) encoding. The six-bit symbols at the output of the Reed-Solomon encoder undergo serial-to-parallel conversion to two three-bit symbols, which are then independently transmitted on the in-phase (I) and quadrature (Q) component of the carrier using 8-*ary* biorthogonal keying (8-BOK). This system has a null-to-null bandwidth of $0.993R_b$, which is 0.7% smaller than TCM with $r = 2/3$ convolutional encoding and 8-PSK modulation. The two waveforms are compared for the relatively benign case where additive white Gaussian noise (AWGN) is the only noise present as well as when pulse-noise interference (PNI) is present. It was found that both systems have almost the same performance in AWGN, but with PNI the alternative system has better performance.			
14. SUBJECT TERMS Trellis Code Modulation, M-ary Bi-Orthogonal Keying, Reed-Solomon Coding, Additive White Gaussian Noise, Pulse Noise Interference, Error-and-Erasure Decoding			**15. NUMBER OF PAGES** 59
			16. PRICE CODE
17. SECURITY CLASSIFICATION OF REPORT Unclassified	**18. SECURITY CLASSIFICATION OF THIS PAGE** Unclassified	**19. SECURITY CLASSIFICATION OF ABSTRACT** Unclassified	**20. LIMITATION OF ABSTRACT** UU

THIS PAGE INTENTIONALLY LEFT BLANK

PERFORMANCE ANALYSIS OF AN ALTERNATIVE TO TRELLIS CODED MODULATION FOR WAVEFORMS TRANSMITTED OVER A CHANNEL WITH PULSE-NOISE INTERFERENCE

Mario Rui Monteiro Marques
Lieutenant, Portuguese Navy
B.S., Portuguese Naval Academy, 2000

Submitted in partial fulfillment of the
requirements for the degrees of

MASTER OF SCIENCE IN ELECTRICAL ENGINEERING
and
MASTER OF SCIENCE IN ELECTRONIC WARFARE SYSTEM ENGINEERING

from the

NAVAL POSTGRADUATE SCHOOL
June 2008

Author: Mario Rui Monteiro Marques

Approved by: Clark Robertson
                 Thesis Advisor

                 Tri Ha
                 Second Reader

                 Jeffrey Knorr
                 Chairman, Department of Electrical and Computer Engineering

                 Dan C. Boger
                 Chairman, Department of Information Sciences

iii

THIS PAGE INTENTIONALLY LEFT BLANK

ABSTRACT

The performance of a communication system having almost the same spectral efficiency as a trellis coded modulation (TCM) system with $r = 2/3$ convolutional encoding and 8-*ary* phase-shift keying (8-PSK) modulation is investigated. TCM is a common solution to the problem of adding forward error correction (FEC) coding without an attendant increase in channel bandwidth. The primary drawback to TCM is that the achievable coding gain is limited by the maximum practical number of states in the convolutional encoder. The alternative system considered uses (63, 37) Reed-Solomon (RS) encoding. The six-bit symbols at the output of the Reed-Solomon encoder undergo serial-to-parallel conversion to two three-bit symbols, which are then independently transmitted on the in-phase (I) and quadrature (Q) component of the carrier using 8-*ary* biorthogonal keying (8-BOK). This system has a null-to-null bandwidth of $0.993R_b$, which is 0.7% smaller than TCM with $r = 2/3$ convolutional encoding and 8-PSK modulation. The two waveforms are compared for the relatively benign case where additive white Gaussian noise (AWGN) is the only noise present as well as when pulse-noise interference (PNI) is present. It was found that both systems have almost the same performance in AWGN, but with PNI the alternative system has better performance.

THIS PAGE INTENTIONALLY LEFT BLANK

TABLE OF CONTENTS

LIST OF FIGURES

THIS PAGE INTENTIONALLY LEFT BLANK

LIST OF TABLES

THIS PAGE INTENTIONALLY LEFT BLANK

EXECUTIVE SUMMARY

The performance of a communication system having almost the same spectral efficiency as a trellis coded modulation (TCM) system with $r = 2/3$ convolutional encoding and 8-*ary* phase-shift keying (8-PSK) modulation is investigated. TCM is a common solution to the problem of adding forward error correction (FEC) coding without an attendant increase in channel bandwidth. The primary drawback to TCM is that the achievable coding gain is limited by the maximum practical number of states in the convolutional encoder. The alternative system considered uses (63, 37) Reed-Solomon (RS) encoding. The six-bit symbols at the output of the Reed-Solomon encoder undergo serial-to-parallel conversion to two three-bit symbols, which are then independently transmitted on the in-phase (I) and quadrature (Q) component of the carrier using 8-*ary* biorthogonal keying (8-BOK). This system has a null-to-null bandwidth of $0.993R_b$, which is 0.7% smaller than TCM with $r = 2/3$ convolutional encoding and 8-PSK modulation. The effect of both AWGN and PNI on the alternative waveform are investigated and compared to the effect of the same type of noise on a TCM signal.

In AWGN, the alternative system requires $E_b / N_o = 5.5$ dB to achieve $P_b = 10^{-5}$ as compared to 5.3 dB for TCM. When PNI is also present, as E_b / N_0 increases, the relative degradation due to PNI increases. This seemingly counterintuitive result can be understood by noting that, while relative performance in PNI is degraded when E_b / N_0 increases, absolute performance is improved. When $E_b / N_0 = 5.6$ dB, $E_b / N_I = 17.8$ dB is required for $P_b = 10^{-5}$, while when $E_b / N_0 = 6.1$ dB, only 0.5 dB more, $E_b / N_I = 14.2$ dB is required for $P_b = 10^{-5}$. This trend continues as E_b / N_0 increases, as can be seen from the results obtained when $E_b / N_0 = 10$ dB, where the maximum degradation due to PNI is 2.8 dB, but $E_b / N_I < 10$ dB is required for $P_b = 10^{-5}$. For realistic values of E_b / N_0, the performance of a TCM system with a comparable spectral efficiency when PNI is present is inferior to the performance of the alternative waveform by about 1.1 dB in terms of E_b / N_I.

The performance of complex 8-BOK with a (63, 37) RS code and errors-and-erasures decoding was also investigated. The benefit of errors-and-erasures decoding when only AWGN is present is negligible, but when PNI is also present, errors-and-erasures decoding improves performance by about 1.6 dB.

ACKNOWLEDGMENTS

THIS PAGE INTENTIONALLY LEFT BLANK

I.   INTRODUCTION

A.   OBJECTIVES

Error control coding can significantly improve communication system performance, but traditional error correction coding either increases bandwidth or reduces throughput. Trellis-coded modulation (TCM) is a technique that implements forward error correction coding without increasing the channel signal bandwidth or decreasing the data rate. With TCM, error control coding, or channel coding, and modulation are treated as a combined operation rather than two separate operations. The number of channel bits is increased by increasing the signal constellation size in order to achieve error correction coding with TCM. In this manner, the information bit rate and the bandwidth remain constant even though the data stream now consists of both data and parity bits [1]. The disadvantage of TCM is that for high data rates a high rate convolutional code is required. Since practical Viterbi decoding techniques limit the number of convolutional code states to 2^8, achievable coding gain is also limited. In this thesis, an alternative system having virtually the same data rate and bandwidth as a TCM system with 8-ary modulation is examined.

The Bose Chaudhuri Hocquenghem (BCH) codes are the most commonly used block codes for random error correction. These codes are cyclic codes and can provide a large selection of block lengths and code rates. The block lengths of several hundred binary BCH codes outperform all other binary block codes having the same block length and code rate. Reed-Solomon codes are nonbinary BCH codes where m bits at a time are combined to form a symbol. An (n, k) RS encoder takes k information symbols (mk information bits) and generates n coded symbols (mn coded bits) [2].

The alternative system to be considered uses (63, 37) Reed-Solomon (RS) encoding. The six-bit symbols at the output of the Reed-Solomon encoder undergo serial-to-parallel conversion to two three-bit symbols, which are then independently transmitted on the in-phase (I) and quadrature (Q) component of the carrier using 8-*ary* biorthogonal keying (8-BOK) [2].

TCM has been examined for additive white Gaussian noise (AWGN) and pulse-noise interference (PNI) [3] but, to the best of the author's knowledge, the alternative system examined in this thesis has never been analyzed before.

B.   THESIS OUTLINE

Apart from Chapter I, the introduction, there are six more chapters. In Chapter II, some background theory is presented. The performance of 8-BOK with a (63, 37) RS code and AWGN is presented in Chapter III. The performance of 8-BOK with a (63, 37) RS code and PNI is discussed in Chapter IV. The performance of 8-BOK with a (63, 37) RS code and errors-and-erasures decoding, is presented in Chapter V. In Chapter VI, the results obtained for TCM are compared to those obtained for 8-BOK with a (63, 37) RS code. Chapter VII is a summary of the thesis and makes recommendations for future work.

II.   BACKGROUND

In this chapter, some background knowledge and concepts required for subsequent analysis are introduced.

A.   SYSTEM DETAIL

A block diagram of the system to be considered is shown in Figure 1 and uses (63, 37) RS encoding. The six-bit symbols at the output of the RS encoder undergo serial-to-parallel conversion to two three-bit symbols, which are then independently transmitted on the in-phase (I) and quadrature (Q) component of the carrier using 8-ary biorthogonal keying (8-BOK).
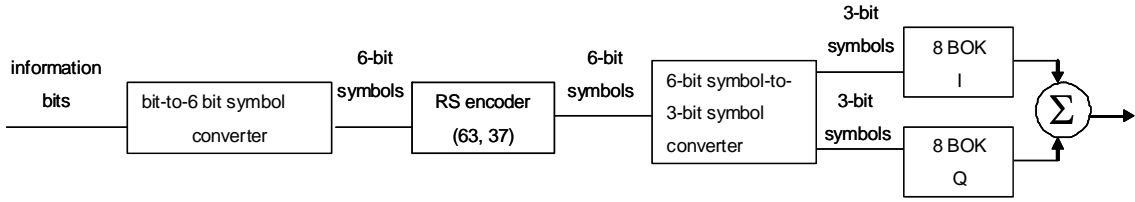
Figure 1.   Transmitter block diagram of complex 8-BOK with (63, 37) RS encoding.

The null-to-null bandwidth of a TCM system implemented with 8-PSK is given by [4]

$$B_{TCM} = R_b \tag{2.1}$$

where R_b is the information bit rate. The null-to-null bandwidth of the alternative system considered in this thesis is [4]

$$B_{nn} = \frac{7}{12} R_{b_c} \tag{2.2}$$

where R_{b_c} is the channel bit rate. For an *(n, k)* block code,

$$R_{b_c} = \frac{n}{k} R_b \tag{2.3}$$

substituting (2.3) into (2.2) we get:

$$B_{nn} = \frac{7n}{12k} R_b \qquad (2.4)$$

in order for $B_{TCM} \approx B_{nn}$, we require

$$\frac{7n}{12k} \approx 1 . \qquad (2.5)$$

For a Reed Solomon code, if we choose $n = 63$, then $k = 37$, yields $B_{nn} \approx 0.99R_b$, which is slightly less than the bandwidth of the spectrally equivalent TCM system.

B.   *M*-ARY BIORTHOGONAL SIGNALS

A set of M symbols can be represented by *M*/2 orthogonal signals by including the negatives of each of the orthogonal signals. Thus, a biorthogonal set is really two sets of orthogonal signal such that each signal in one set has its antipodal signal in the other. One advantage of biorthogonal modulation over orthogonal modulation for the same data rate is that biorthogonal modulation requires one-half as many chips per symbol when baseband orthogonal waveforms are used. Thus, the bandwidth requirement for biorthogonal modulation is one-half of that required for comparable orthogonal modulation that uses baseband orthogonal waveforms. Since antipodal signal vectors have better distance properties than orthogonal ones, biorthogonal modulation performs slightly better than orthogonal modulation [5].

The channel waveform for complex *M*BOK can be represented by

$$s(t) = \pm A_c \cos\left(2\pi f_m t + \theta\right) - \left(\pm\right) A_c \sin\left(2\pi f_n t + \theta\right) \qquad (2.6)$$

which is transmitted for $T_s = 2kT_b$ seconds , $2k$ is the number of bits in each symbol, and $f_x(t)$, *x=m, n, x=1,2,…,M*/2, are the orthogonal signaling frequencies, where *m* and *n* may, or may not, be different depending on the data bits. Clearly, complex 2^k-BOK is equivalent to transmitting 2^k-BOK independently on both the I and Q components of the carrier, so complex 2^k-BOK is actually a 2^{2k}-ary modulation technique.

4

A block diagram of a *M*-ary biorthogonal receiver for the I-signal component is shown in Figure 2. The block diagram for the Q-signal component is identical except that the local oscillators are in phase quadrature to those shown in Figure 2.
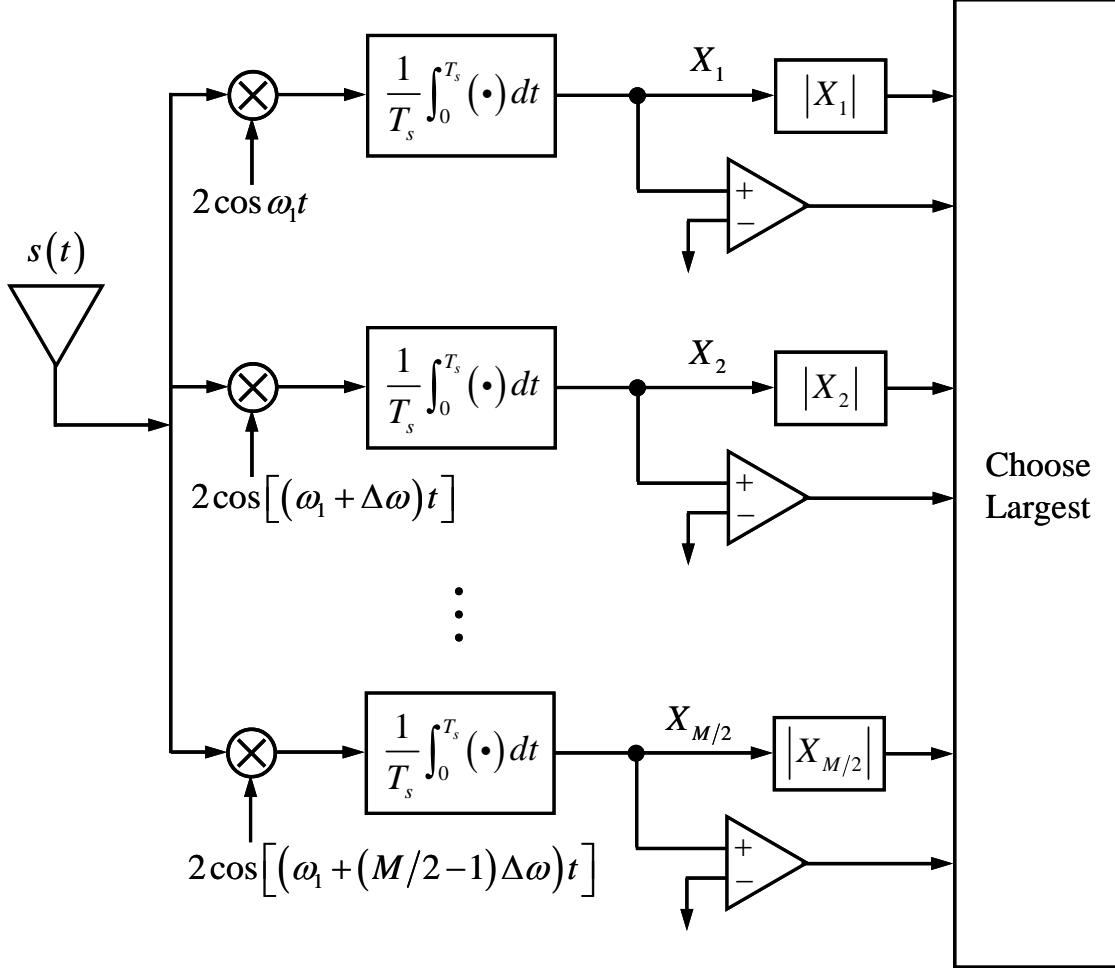
Figure 2.   Block diagram of a *M*-ary biorthogonal receiver for the I-signal component.

C.   PERFORMANCE OF *MBOK* IN AWGN

When AWGN is present, the total received signal is given by [5]

$$s(t) = \pm A_c \cos(2\pi f_m t + \theta) - (\pm) A_c \sin(2\pi f_n t + \theta) + n(t). \qquad (2.7)$$

Since the I and Q signals are independent, the probability of symbol error is the same for I and Q. Without loss of generality, we can obtain the probability of I symbol error P_{S_I}.

The conditional probability density function for the random variables X_m, where $m = 1, 2, ..., M/2$, that represents the integrator outputs when the noise can be considered Gaussian noise is given by [5]

$$f_{X_m}(x_m \mid m) = \frac{1}{\sqrt{2\pi}\sigma} \exp\left[\frac{-\left(x_m - \sqrt{2}A_c\right)^2}{2\sigma^2}\right] \quad \text{for } m \leq M/2 \tag{2.8}$$

$$f_{X_m}(x_m \mid m) = \frac{1}{\sqrt{2\pi}\sigma} \exp\left[\frac{-\left(x_m + \sqrt{2}A_c\right)^2}{2\sigma^2}\right] \quad \text{for } M/2 + 1 \leq m \leq M \tag{2.9}$$

and

$$f_{X_n}(x_n \mid n, \, n \neq m) = \frac{1}{\sqrt{2\pi}\sigma} \exp\left[\frac{-x_n^2}{2\sigma^2}\right] \tag{2.10}$$

where $\sigma^2 = N_0/T_s$, and the probability of channel symbol error for M-ary biorthogonal keying (MBOK) in AWGN is [4]

$$P_{S_I} = 1 - \frac{1}{\sqrt{2\pi}} \int_{-\sqrt{2E_s/N_0}}^{\infty} e^{\frac{-u^2}{2}} \left[1 - 2Q\left(u + \sqrt{\frac{2E_s}{N_0}}\right)\right]^{\frac{M}{2}-1} du \tag{2.11}$$

where E_s is the average energy per channel symbol, $E_s = A_c^2 T_s$, where A_c^2 is the average received signal power, T_s is the symbol duration, and $Q(\bullet)$ is the Q-function.

The union bound for MBOK in AWGN is [4]

$$P_{S_I} \leq (M-2)Q\left(\sqrt{\frac{E_s}{N_o}}\right) + Q\left(\sqrt{\frac{2E_s}{N_o}}\right). \tag{2.12}$$

As previously mentioned, the probability of Q symbol error $P_{S_I} = P_{S_Q}$.

D. PERFORMANCE OF *MBOK* IN AWGN WITH PULSED-NOISE INTERFERENCE

When a channel is affected by AWGN, the noise signal that arrives at the receiver is assumed to be uniformly spread across the spectrum and time-independent. When there is PNI in the channel, the preceding assumptions are not valid. The total noise power at the receiver integrator outputs when both AWGN and PNI are present is given by

$$\sigma_X^2 = \sigma_o^2 + \sigma_I^2 \qquad (2.13)$$

where $\sigma_o^2 = N_0 / T_b$, $\sigma_I^2 = N_I / \rho T_b$, and ρ $(0 < \rho \leq 1)$ is the fraction of time that a narrowband Gaussian noise interferer is switched on. In the event $\rho = 1$, the PNI is considered barrage noise interference since it is on continuously.

If we assume that a channel symbol either experience PNI or it does not, then the probability of symbol error when a signal experiences PNI can be expressed by

$$P_{S_I} = Pr\,(\text{PNI})\,P_{S_I}\,(\text{PNI}) + \ Pr\,(\text{AWGN})\,P_{S_I}\,(\text{AWGN}) \qquad (2.14)$$

which is given by

$$P_{S_I} = \rho\,P_{S_I}\,(PNI) + (1 - \rho)\,P_{S_I}\,(\text{AWGN}) \qquad (2.15)$$

where $P_{S_I}(x)$ represent the probability of symbol error for condition x. As mentioned, equation (2.15) is derived by assuming that a symbol is either completely free of interference or is interfered with for an entire symbol.

E. ERROR CORRECTION CODING

Implementing error control coding can significantly improve communication system performance. F*orward error correction coding* (FEC) consists of adding a certain number of redundant bits to the actual data bits in particular pattern such that recovery of the actual data bits is enhanced.

As mentioned in Chapter I, the system under consideration in this thesis incorporates a Reed-Solomon, nonbinary block code for FEC. For a *(n,k)* RS code, the probability of decoder error, or block error, is upper bounded by the sum of the probabilities that a received code word differs from the correct code word by i symbols for all $i > t$ [2]. Therefore,

$$P_E \leq \sum_{i=t+1}^{n} \binom{n}{i} p_s^{\ i} (1 - p_s)^{n-i} \qquad (2.16)$$

or

$$P_E \leq 1 - \sum_{i=0}^{t} \binom{n}{i} p_s^{\ i} (1 - p_s)^{n-i} \qquad (2.17)$$

where the inequality holds for either a perfect code or a bounded distance decoder, p_s is the channel symbol error probability and t is the symbol-error correcting capability of the code. The probability of information symbol error is given by [4]

$$P_s \approx \frac{1}{n} \sum_{i=t+1}^{n} i \binom{n}{i} p_s^{\ i} (1 - p_s)^{n-i}. \qquad (2.18)$$

The probability of bit error can be approximated by taking the average of the upper and lower bounds [4]. Hence,

$$P_b \approx \left(\frac{m+1}{2m} \right) P_s. \qquad (2.19)$$

F.   ERRORS-AND-ERASURES DECODING

The simplest form of soft decision decoding is error-and-erasures (EED). In binary erasure decoding, the output of the demodulator has three possible outputs 1, 0 and erasure (e). Presume that a received code word has a single erased bit. Now all valid code words are separated by a Hamming distance of at least $d_{\min} - 1$, where $d_{\min}$ is the minimum Hamming distance of the code. In general, given e erasures in a received code word, all valid code words are separated by a Hamming distance of at least $d_{\min} - e$. Consequently, the effective free distance between valid code words when there are e erasures in the received code word is given by [2]

8

$$d_{\min_{eff}} = d_{\min} - e.$$ (2.20)

Therefore, the number of errors in the non-erased bits of the code word that can be corrected is given by [5]

$$t_e = \left\lfloor \frac{d_{\min} - e - 1}{2} \right\rfloor$$ (2.21)

where $\lfloor x \rfloor$ implies rounding x down. We can correct t_e errors and e erasures as long as

$$2t_e + e < d_{\min}.$$ (2.22)

Hence, twice as many erasures as errors can be corrected. Intuitively, this makes sense because we have more information about the erasures; the locations of the erasures are known, but the locations of the errors are not.

For error-and-erasures decoding, the probability that there are a total of i errors and j erasures in a block of n symbols is given by [2]

$$\Pr(i, j) = \binom{n}{i}\binom{n-i}{j} p_s^i p_e^j p_c^{n-i-j}$$ (2.23)

where each symbol is assumed to be received independently, p_e is the probability of channel symbol erasure, p_s is the probability of channel symbol error, and p_c is the probability of correct channel symbol detection. The probability of channel error can be obtained from [2]

$$p_s = 1 - p_e - p_c.$$ (2.24)

Since a block error does not occur as long as $d_{\min} > 2i + j$, then the probability of correct block decoding is given by [2]

$$P_C = \sum_{i=0}^{t} \binom{n}{i} p_s^i \sum_{j=0}^{d_{\min}-1-2i} \binom{n-i}{j} p_e^j p_c^{n-i-j}.$$ (2.25)

Now the probability of block error is given by [2]

$$P_E = 1 - P_C \qquad (2.26)$$

which is

$$P_E = 1 - \sum_{i=0}^{t} \binom{n}{i} p_s^i \sum_{j=0}^{d_{\min}-1-2i} \binom{n-i}{j} p_e^j p_c^{n-i-j}. \qquad (2.27)$$

Using the average of the upper and lower bound on the probability of symbol error given that a block error has occurred, we can approximate the probability of symbol error as

$$P_s \approx \left(\frac{k+1}{2k} \right) P_E. \qquad (2.28)$$

For a block code that can correct up to t symbol errors in every block of n symbols, with errors and erasures decoding, a block error occurs when $i > t$ regardless of the value of j or if $j > (d_{\min} - 1 - 2i)$ even when $i \le t$. As a result [2]

$$P_E = \sum_{i=t+1}^{n} \binom{n}{i} p_s^i \sum_{j=0}^{n-i} \binom{n-i}{j} p_e^j p_c^{n-i-j} + \sum_{i=0}^{t} \binom{n}{i} p_s^i \sum_{j=d_{\min}-2i}^{n-i} \binom{n-i}{j} p_e^j p_c^{n-i-j}. \qquad (2.29)$$

From the approximation for the conditional probability of symbol error given a block error [4] and the preceding expression for the probability of block error,

$$P_s \approx \frac{1}{n} \left[\sum_{i=t+1}^{n} \binom{n}{i} p_s^i \sum_{j=0}^{n-i} (i+j) \binom{n-i}{j} p_e^j p_c^{n-i-j} + \sum_{i=0}^{t} \binom{n}{i} p_s^i \sum_{j=d_{\min}-2i}^{n-1} (i+j) \binom{n-i}{j} p_e^j p_c^{n-i-j} \right]. \qquad (2.30)$$

G.   CHAPTER SUMMARY

In this chapter, biorthogonal signals and the background and concepts necessary to examine the performance of *MBOK* in AWGN and PNI were introduced. The concept of error correction coding and some analysis of the performance of *MBOK* were also examined.

In the next chapter, the performance of the alternative waveform with complex 8-BOK and (63, 37) RS coding in AWGN is investigated.

10

III. PERFORMANCE OF THE ALTERNATIVE WAVEFORM IN AWGN

In this chapter, the performance of the alternative waveform with complex 8-BOK and (63, 37) RS coding is investigated. As a first step, the results obtained using the exact expression are compared to those obtained with the upper bound.

A. COMPARISON OF THE EXACT AND THE UPPER BOUND RESULTS FOR THE PROBABILITY OF SYMBOL ERROR IN AWGN

From (2.6) with $m=8$,

$$P_{S_I} = 1 - \frac{1}{\sqrt{2\pi}} \int_{-\sqrt{\frac{6rE_b}{N_0}}}^{\infty} \exp\left(\frac{-u^2}{2}\right) \cdot \left[1 - 2Q\left(u + \sqrt{\frac{6rE_b}{N_0}}\right)\right]^3 du \qquad (3.1)$$

where $r=37/63$. From (2.12), an upper bound on the probability of symbol error with $m=8$ is

$$P_{S_I} \leq 6Q\left(\sqrt{\frac{3rE_b}{N_o}}\right) + Q\left(\sqrt{\frac{6rE_b}{N_o}}\right). \qquad (3.2)$$

Equations (3.1) and (3.2) vs. E_b/N_0 are plotted in Figure 3. As can be seen, for $P_{S_I} < 10^{-3}$ the exact and the upper bound results are indistinguishable.
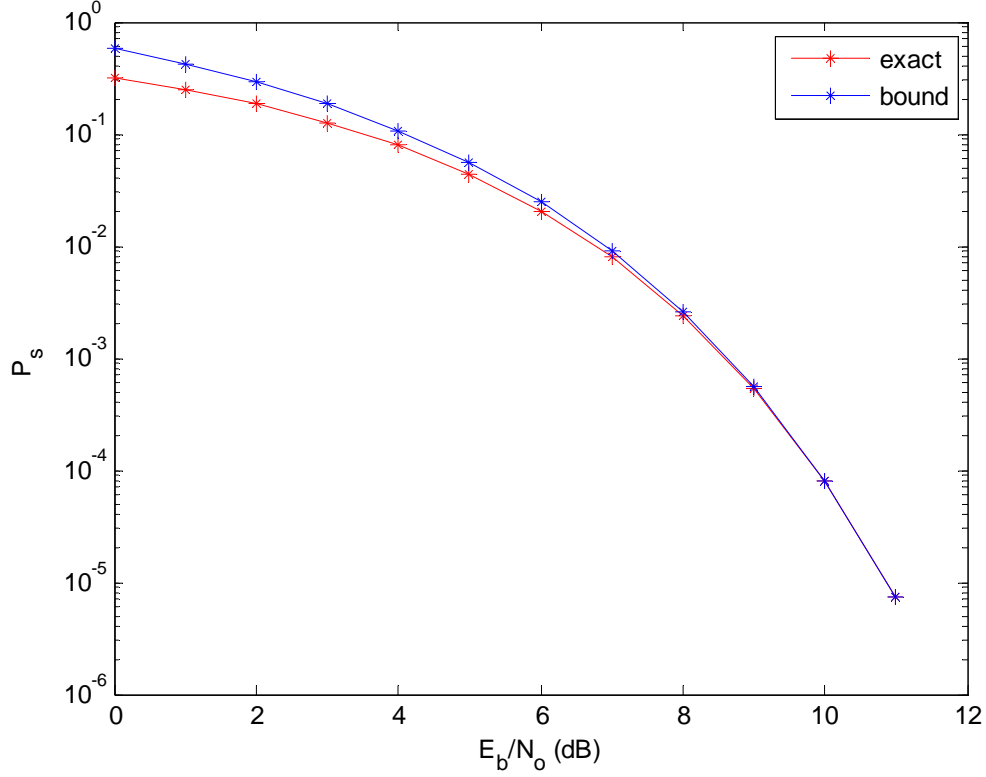
Figure 3. The exact and the upper bound for the probability of symbol error of 8-BOK in AWGN.

B. PERFORMANCE OF COMPLEX 8-BOK WITH A (63, 37) RS CODE IN AWGN

In order to obtain the performance of the system under consideration, the probability of I and Q symbol error must be related to the overall probability of symbol error. Since the probability of correct symbol detection for I and Q are the same, then

$$p_{C_I} = p_{C_Q} = 1 - p_{S_I} = 1 - p_{S_Q}. \tag{3.3}$$

The overall probability of correct symbol detection is given by

$$p_C = p_{C_I} \cap p_{C_Q} = p_{C_I} p_{C_Q} \tag{3.4}$$

since, in order for a symbol to be received correctly, both the I and Q symbols must be received correctly and since p_{C_I} and p_{C_Q} are independent. Substituting (3.3) into (3.4), we get

$$p_C = \left(1 - p_{S_I}\right)^2. \tag{3.5}$$

Since

$$p_S = 1 - p_C \tag{3.6}$$

then, substituting (3.5) into (3.6), we get

$$p_S = 1 - \left(1 - 2p_{SI} + p_{SI}^2\right). \tag{3.7}$$

Equation (3.7) can be simplified to obtain

$$p_S = p_{SI}\left(2 - p_{SI}\right). \tag{3.8}$$

The results from (3.2) are used in (3.8), and these results are used in (2.18) and (2.19) to obtain the results for the alternative waveform in AWGN. The results are shown in Figure 4. As we see from Figure 4, at $P_b = 10^{-5}$ the alternative system requires $E_b / N_o = 5.5$ dB.

C.   CHAPTER SUMMARY

In this chapter, the results obtained using the exact expression and the upper bound for the probability of symbol error in AWGN was compared. Next, the probability of bit error vs. E_b / N_0 for AWGN for the alternative system was examined.

In the next chapter, the performance of the alternative waveform with complex 8-BOK and (63, 37) RS coding in PNI is investigated.
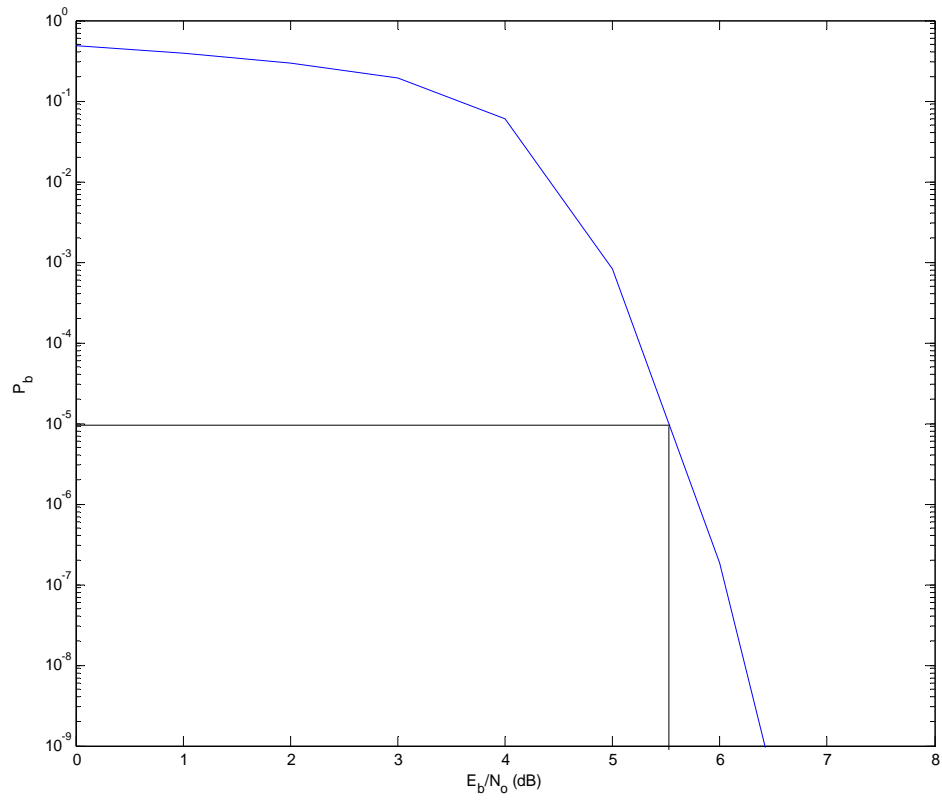
Figure 4.   Performance of complex 8-BOK with a (63, 37) RS code in AWGN.

IV. PERFORMANCE OF THE ALTERNATIVE WAVEFORM IN PNI

In this chapter, the performance of complex 8-BOK with a (63, 37) RS code is investigated by analyzing the probability of bit error vs. E_b / N_I. First, the results obtained using the exact expression and the upper bound are compared.

A. COMPARISON OF THE EXACT AND THE UPPER BOUND RESULTS FOR THE PROBABILITY OF SYMBOL ERROR IN PNI

The exact expression for the probability of I channel symbol error for the alternative waveform is

$$p_{S_I} = \rho p_{S_{I_I}} + (1 - \rho) p_{S_{I_0}} \tag{4.1}$$

where $p_{S_{I_0}}$ is given by (3.1) and $p_{S_{I_I}}$ is obtained by replacing E_b / N_0 with

$$\frac{E_b}{N_0 + \dfrac{N_I}{\rho}} = \frac{3}{\left(\dfrac{E_b}{N_o} \right)^{-1} + \dfrac{1}{\rho} \left(\dfrac{E_b}{N_I} \right)^{-1}} \tag{4.2}$$

in (3.1) to obtain:

$$. \, p_{S_{I_I}} = 1 - \frac{1}{\sqrt{2\pi}} \int_{-\sqrt{\frac{6r}{\left(\frac{E_b}{N_0} \right)^{-1} + \frac{1}{\rho} \left(\frac{E_b}{N_I} \right)^{-1}}}}^{\infty} e^{\frac{-u^2}{2}} \left[1 - 2Q \left(u + \sqrt{\frac{6r}{\left(\frac{E_b}{N_0} \right)^{-1} + \frac{1}{\rho} \left(\frac{E_b}{N_I} \right)^{-1}}} \right) \right]^3 du . \tag{4.3}$$

The results from (4.1) are used in (3.8), and these results are used in (2.18) and (2.19) to obtain the results shown in Figure 5.

Similarly, the upper bound given by (3.2) can be adapted when PNI is present to obtain

$$p_{S_I} = \rho \left[6Q \left(\sqrt{\dfrac{3r}{\sqrt{\left(\dfrac{E_b}{N_0}\right)^{-1} + \left(\dfrac{E_b}{N_I}\right)^{-1} \dfrac{1}{\rho}}}} \right) + Q \left(\sqrt{\dfrac{6r}{\sqrt{\left(\dfrac{E_b}{N_0}\right)^{-1} + \left(\dfrac{E_b}{N_I}\right)^{-1} \dfrac{1}{\rho}}}} \right) \right] + (1-\rho) \left[6Q \left(\sqrt{\dfrac{3rE_s}{N_o}} \right) + Q \left(\sqrt{\dfrac{6rE_s}{N_o}} \right) \right] \quad (4.4)$$

which is used in the same manner as (4.3) to obtain the upper bound results shown in Figure 5.
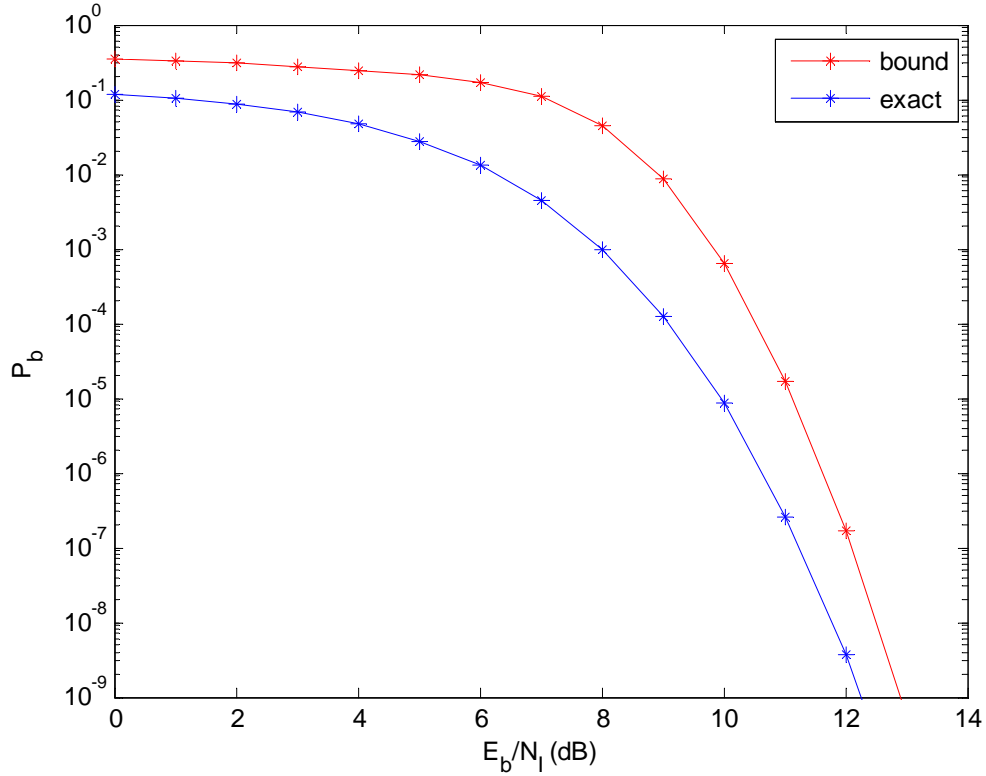
Figure 5.   The exact and the upper bound results for the probability of symbol error with PNI for $\rho = 0.1$.

As can be seen, for $P_b = 10^{-5}$ the exact and the upper bound results are about 1 dB apart. Hence, the exact equation is used to calculate the probability of symbol error with PNI.

B.   PERFORMANCE OF 8-BOK WITH A (63, 37) RS CODE IN PNI

The results from (4.3) are used in (3.8), and the (3.8) results are used in (2.18) and (2.19) to obtain the results shown in Figures 6, 7 and 8.

16

Figure 6.   Performance of complex 8-BOK with a (63, 37) RS code and PNI for
$E_b / N_0 = 5.6$ dB.

The results are summarized in Table 1, where the E_b / N_0 was selected
for $P_b = 10^{-6}$ when $E_b / N_I \gg 1$. As can be seen, PNI with $\rho = 0.1$ degradates
performance by an additional 0.8 dB as compared to continuous noise interference
$(\rho = 1.0)$.

Table 1.   Performance of complex 8-BOK with a (63, 37) RS code and PNI
for $P_b = 10^{-5}$ with $E_b / N_0 = 5.6$ dB.

ρ	E_b / N_I
$\rho = 1$	17.0 dB
$\rho = 0.2$	17.5 dB
$\rho = 0.1$	17.8 dB
$\rho = 0.02$	16.8 dB
$\rho = 0.01$	9.4 dB

Generally, we conclude that, up to a point, as ρ decreases the performance of the alternative system degrades. Then, as ρ continues to decrease, the alternative system performance begins to improve.
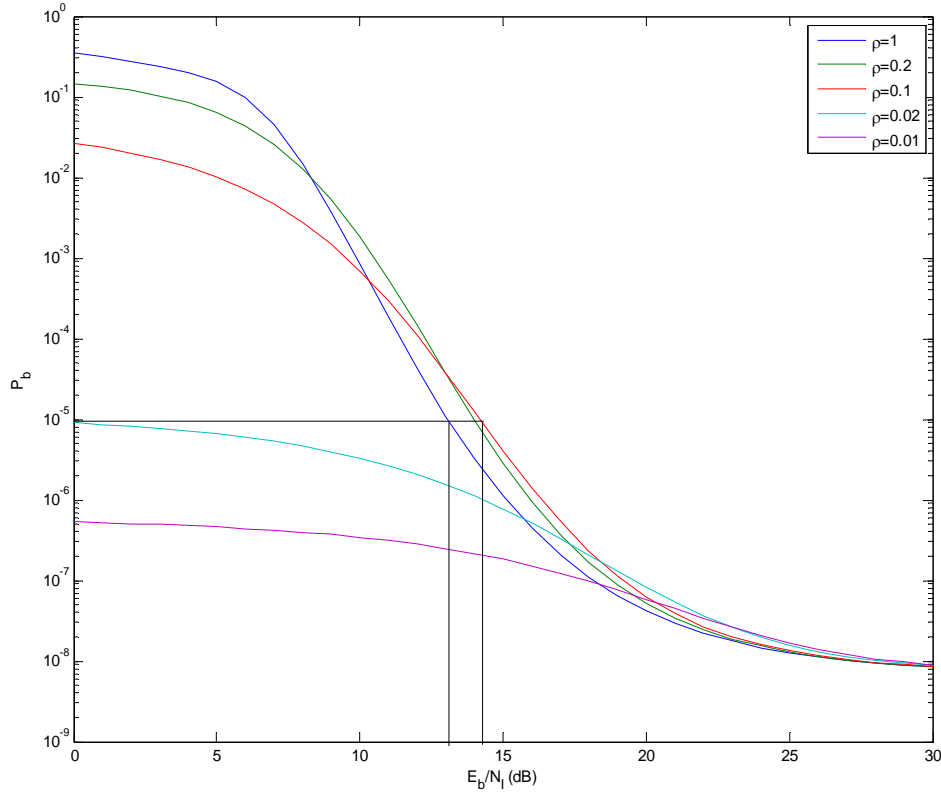
Figure 7.   Performance of complex 8-BOK with a (63, 37) RS code and PNI for
$E_b / N_0 = 6.1$ dB.

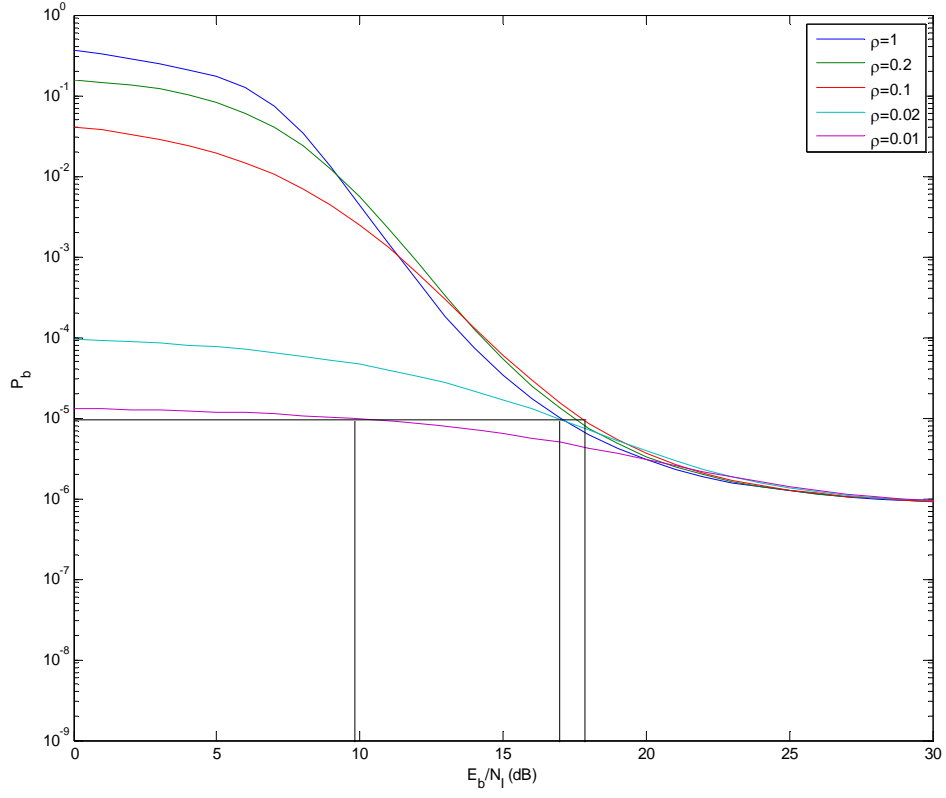The results are summarized in Table 2, where the E_b / N_0 was selected for $P_b = 10^{-8}$ when $E_b / N_I \gg 1$. In this case, PNI with $\rho = 0.1$ degrades performance by an additional 1.1 dB as compared to $\rho = 1.0$. Hence, as E_b / N_0 increases, the relative degradation due to PNI increases. This seemingly counterintuitive result can be understood by noting that, while relative performance in PNI is degraded when E_b / N_0 increases, absolute performance is improved. When $E_b / N_0 = 5.6$ dB, $E_b / N_I = 17.8$ dB is required for $P_b = 10^{-5}$, while when $E_b / N_0 = 6.1$ dB, only 0.5 dB more, $E_b / N_I = 14.2$ dB is required for $P_b = 10^{-5}$. This trend continues as E_b / N_0 increases, as can be seen from the result obtained when $E_b / N_0 = 10$ dB, shown in Figure 8 and summarized in Table 3.

19

Table 2.   Performance of complex 8-BOK with a (63, 37) RS code and PNI
for $P_b = 10^{-5}$ with $E_b / N_0 = 6.1$ dB.

ρ	E_b / N_I
$\rho = 1$	13.1 dB
$\rho = 0.2$	14.0 dB
$\rho = 0.1$	14.2 dB
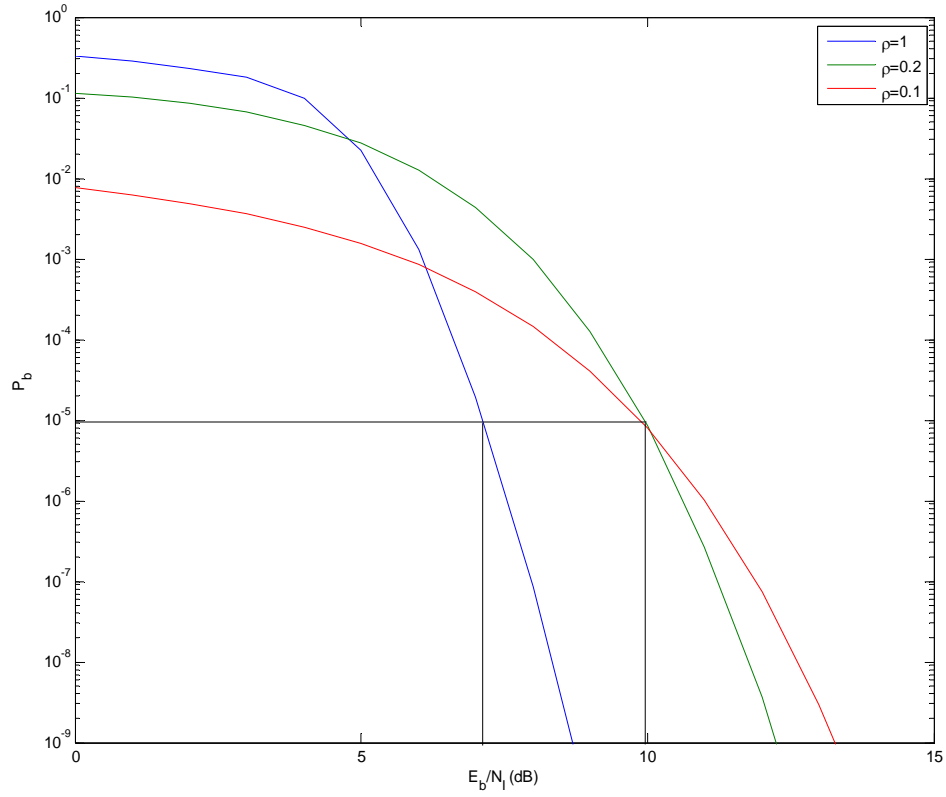
Figure 8.   Performance of complex 8-BOK with a (63, 37) RS code and PNI for
$E_b / N_0 = 10.0$ dB.

Table 3.   Performance of complex 8-BOK with a (63, 37) RS code and PNI
for $P_b = 10^{-5}$ with $E_b / N_0 = 10.0$ dB.

ρ	E_b / N_I
$\rho = 1$	7.1 dB
$\rho = 0.2$	9.9 dB
$\rho = 0.1$	9.8 dB

In this case, the maximum degradation due to PNI is 2.8 dB, but now $E_b / N_I < 10$ dB required for $P_b = 10^{-5}$.

C.   CHAPTER SUMMARY

In this chapter, the results obtained from the exact expression and the upper bound for the probability of symbol error in PNI was compared. Next, the probability of bit error vs. E_b / N_I for complex 8-BOK with a (63, 37) RS code was analyzed when PNI was present. The ratio E_b / N_0 was selected such that $P_b = 10^{-6}$, 10^{-8} and 10^{-40} when $E_b / N_I \gg 1$ in order to examine the effect of AWGN when PNI is also present.

In the next chapter, the performance of complex 8-BOK with a (63, 37) RS code and errors-and-erasures decoding is investigated.

THIS PAGE INTENTIONALLY LEFT BLANK

V. PERFORMANCE OF COMPLEX 8-BOK WITH A (63, 37) RS CODE AND ERRORS-AND-ERASURES DECODING

In this chapter, the performance of complex 8-BOK with a (63, 37) RS code and errors-and-erasures decoding is investigated for both AWGN alone and AWGN and PNI together.

A. PERFORMANCE OF COMPLEX 8-BOK WITH A (63, 37) RS CODE WITH ERRORS-AND-ERASURES DECODING

For *MBOK*, the probability of symbol erasure is given by [4]

$$p_{e_0} = \left[Q\left(\frac{\sqrt{2}A_c - V_T}{\sigma} \right) - Q\left(\frac{V_T + \sqrt{2}A_c}{\sigma} \right) \right] \left[1 - 2Q\left(\frac{V_T}{\sigma} \right) \right]^{0.5M-1}. \tag{5.1}$$

Substituting $V_T = a\sqrt{2}A_c$ and $\sigma^2 = \dfrac{N_0}{T_{bc}} = \dfrac{N_0}{rT_b}$ into (5.1), we obtain for 8-BOK:

$$p_{e_I} = \left\{ Q\left[(1-a)\sqrt{\frac{6rE_b}{N_0}} \right] - Q\left[(1+a)\sqrt{\frac{6rE_b}{N_0}} \right] \right\} \left[1 - 2Q\left(a\sqrt{\frac{6rE_b}{N_0}} \right) \right]^3. \tag{5.2}$$

Following the procedure in Chapter IV when PNI is present, we obtain for 8-BOK

$$p_{e_2} = \left\{ Q\left[(1-a)\sqrt{\frac{6r}{\left(\frac{E_b}{N_0} \right)^{-1} + \left(\frac{E_b}{N_I} \right)^{-1}\frac{1}{\rho}}} \right] - Q\left[(1+a)\sqrt{\frac{6r}{\left(\frac{E_b}{N_0} \right)^{-1} + \left(\frac{E_b}{N_I} \right)^{-1}\frac{1}{\rho}}} \right] \right\} \left[1 - 2Q\left(a\sqrt{\frac{6r}{\left(\frac{E_b}{N_0} \right)^{-1} + \left(\frac{E_b}{N_I} \right)^{-1}\frac{1}{\rho}}} \right) \right]. \tag{5.3}$$

Now substituting (5.2) and (5.3) into

$$p_{e_{I_I}} = \rho p_{e_I} + (1-\rho) p_{e_0}, \tag{5.4}$$

we obtain the overall probability of symbol erasure for the I-signal component.

The probability of correct symbol detection for *MBOK* with errors-and-erasures demodulation is given by [4]

$$P_c = \int_{V_T}^{\infty} \frac{1}{\sqrt{2\pi}\sigma} e^{\left[\frac{-(x_1-\sqrt{2}A_c)^2}{2\sigma^2}\right]} \left[1-2Q\left(\frac{x_1}{\sigma}\right)\right]^{M/2-1} dx_1 .$$ (5.5)

Substituting $V_T = a\sqrt{2}A_c$ and $\dfrac{A_c}{\sigma} = \sqrt{\dfrac{3rE_b}{N_o}}$ into (5.5), we obtain for 8-BOK:

$$p_{c_0} = \int_{-(1-a)\sqrt{\frac{6rE_b}{N_0}}}^{\infty} \frac{1}{\sqrt{2\pi}} e^{-\frac{u^2}{2}} \left[1-2Q\left(u+\sqrt{\frac{6rE_b}{N_0}}\right)\right] du .$$ (5.6)

Again, following the procedure in Chapter IV when PNI is present, we get for 8-BOK:

$$p_{c_I} = \int_{-(1-a)\sqrt{\frac{6r}{\left(\frac{E_b}{N_o}\right)^{-1}+\frac{1}{\rho}\left(\frac{E_b}{N_I}\right)^{-1}}}}^{\infty} \frac{1}{\sqrt{2\pi}} e^{-\frac{u^2}{2}} \left[1-2Q\left(u+\sqrt{\frac{6r}{\left(\frac{E_b}{N_o}\right)^{-1}+\frac{1}{\rho}\left(\frac{E_b}{N_I}\right)^{-1}}}\right)\right]^3 .$$ (5.7)

Substituting (5.6) and (5.7) into

$$p_{c_{I_I}} = \rho p_{c_I} + (1-\rho) p_{c_0} ,$$ (5.8)

we obtain the overall probability of correct symbol detection for the I-signal component.

B. UNION BOUND FOR *MBOK* WITH ERRORS-AND-ERASURES DEMODULATION

In this section, the union bound on the probability of symbol error for *MBOK* with errors-and-erasures demodulation is derived. This derivation is necessary due to numerical difficulties that were encountered in computing the probability of symbol error with errors-and-erasures demodulation from the exact expression given by

$$p_s = 1 - p_e - p_c .$$ (5.9)

We assume without loss of generality that the signal corresponding to symbol $m=1$ is transmitted. From the block diagram of the *MBOK* receiver shown in Figure 2 and assuming that symbol $m=1$ is received only when $X_1 > V_T \cap X_1 > 0$, we see that a

24

symbol error occurs when $X_1 < 0$ or $X_n > V_T \cap X_n > X_1$, $n = 2,\ 3,\ 4,\ldots\ldots,\ M/2$ or

$|X_n| > V_T \cap |X_n| > X_1$, $n = M/2+2,\ M/2+3,\ldots\ldots,\ M$. These conditions can be expressed by

$$P_s = P_r\left(X_2 > V_T \cup X_3 > V_T \cup \ldots\ldots \cup X_{M/2} > V_T \cup |X_{M/2+2}| > V_T \cup \ldots\ldots \cup |X_M| > V_T \,/\, X_1 > 0\right) + P_r\left(X_1 < 0\right). \quad (5.10)$$

Equation (5.10) is upper bounded by

$$P_s < P_r\left(X_2 > V_T \cup X_3 > V_T \cup \ldots\ldots \cup X_{M/2} > V_T \cup |X_{M/2+2}| > V_T \cup \ldots\ldots \cup |X_M| > V_T \,/\, X_1 > 0\right) + P_r\left(X_1 < 0\right). \quad (5.11)$$

Since we assume the X_ms, $m \neq 1$, are identical, independent random variables, we can replace the first part of (5.11) with a union bound to get

$$P_s < 2\left(M/2 - 1\right)P_r\left(X_2 > V_T \,/\, X_1 > 0\right) + P_r\left(X_1 < 0\right). \qquad (5.12)$$

Equation (5.12) can now be expressed in terms of the probability density functions of X_1 and X_2 to get

$$P_s < (M-2)\int_{V_T}^{\infty} f_{X_2}\left(x_2\,/1\right)\left[\int_0^{x_2} f_{X_1}\left(x_1\,/1\right)dx_1\right]dx_2 + \int_{-\infty}^{V_T} f_{X_1}\left(x_1\,/1\right)dx_1. \qquad (5.13)$$

For AWGN, the last part of (5.13) is:

$$\int_{-\infty}^{-V_T} f_{X_1}\left(x_1\,/1\right)dx_1 = \int_{-\infty}^{-V_T} \frac{1}{\sqrt{2\pi}\sigma}e^{-\left(x_1-\sqrt{2}A_c\right)^2/2\sigma^2}dx_1. \qquad (5.14)$$

Substituting $u = \dfrac{x_1 - \sqrt{2}A_c}{\sigma}$ and $du = \dfrac{dx_1}{\sigma}$ into (5.14), we get

$$\int_{-\infty}^{-V_T} f_{X_1}\left(x_1\,/1\right)dx_1 = \int_{-\infty}^{-(V_T+\sqrt{2}A_c)/\sigma} \frac{1}{\sqrt{2\pi}}e^{-u^2/2}du. \qquad (5.15)$$

Now (5.15) can be evaluated to get

$$\int_{-\infty}^{-V_T} f_{X_1}\left(x_1\,/1\right)dx_1 = Q\left(\frac{V_T + \sqrt{2}A_c}{\sigma}\right). \qquad (5.16)$$

Letting $V_T = a\sqrt{2}A_c$ in (5.16), we obtain for the last part of (5.13)

$$\int_{-\infty}^{-V_T} f_{X_1}\left(x_1/1\right)dx_1 = Q\left[\left(1+a\right)\sqrt{\frac{2E_s}{N_o}}\right]. \tag{5.17}$$

The inner integral of the first part of (5.13) can be evaluated in a similar manner to obtain

$$\int_{0}^{x_2} f_{X_1}\left(x_1/1\right)dx_1 = \left[1 - Q\left(\sqrt{\frac{2E_s}{N_0}}\right) - Q\left(\frac{x_2}{\sigma} - \sqrt{\frac{2E_s}{N_0}}\right)\right]. \tag{5.18}$$

Substituting (5.18) into the first part of (5.13), we get

$$\int_{V_T}^{\infty} f_{X_2}\left(x_2/1\right)\left[\int_{0}^{x_2} f_{X_1}\left(x_1/1\right)dx_1\right]dx_2 = \frac{1}{\sqrt{2\pi}\sigma}\int_{V_T}^{\infty} e^{-x_2^2/2\sigma^2}\left[1 - Q\left(\sqrt{\frac{2E_s}{N_0}}\right) - Q\left(\frac{x_2}{\sigma} - \sqrt{\frac{2E_s}{N_0}}\right)\right]dx_2 \tag{5.19}$$

which can be evaluated to obtain

$$\int_{V_T}^{\infty} f_{X_2}\left(x_2/1\right)\left[\int_{0}^{x_2} f_{X_1}\left(x_1/1\right)dx_1\right]dx_2 = Q\left(a\sqrt{\frac{2E_s}{N_0}}\right)\left[1 - Q\left(\sqrt{\frac{2E_s}{N_0}}\right)\right] - \frac{1}{\sqrt{2\pi}}\int_{a\sqrt{\frac{2E_s}{N_o}}}^{\infty} e^{-u^2/2}Q\left(u - \sqrt{\frac{2E_s}{N_0}}\right)du. \tag{5.20}$$

Now substituting (5.20) and (5.17) into (5.13), we obtain

$$P_s < (M-2)\left\{Q\left(a\sqrt{\frac{2E_s}{N_0}}\right)\left[1 - Q\left(\sqrt{\frac{2E_s}{N_0}}\right) - \frac{1}{\sqrt{2\pi}}\int_{a\sqrt{\frac{2E_s}{N_o}}}^{\infty} e^{-u^2/2}Q\left(u - \sqrt{\frac{2E_s}{N_0}}\right)du\right]\right\} + Q\left((1+a)\sqrt{\frac{2E_s}{N_0}}\right). \tag{5.21}$$

C. PERFORMANCE OF THE ALTERNATIVE WAVEFORM WITH ERRORS-AND-ERASURES DECODING

In this section, the probability of bit error for complex *MBOK* with errors-and-erasures demodulation is derived.

Following the procedure used Chapter IV when PNI is present, we get from (5.21)

$$p_{s_{I_I}} < (M-2)\left\{Q\left(a\sqrt{\frac{6r}{\left(\frac{E_b}{N_0}\right)^{-1}+\left(\frac{E_b}{N_I}\right)^{-1}\frac{1}{\rho}}}\right)\left[1-Q\left(\sqrt{\frac{6r}{\left(\frac{E_b}{N_0}\right)^{-1}+\left(\frac{E_b}{N_I}\right)^{-1}\frac{1}{\rho}}}\right)-\frac{1}{\sqrt{2\pi}}\int_{a\sqrt{\frac{6r}{\left(\frac{E_b}{N_0}\right)^{-1}+\left(\frac{E_b}{N_I}\right)^{-1}\frac{1}{\rho}}}}^{\infty}e^{-u^2/2}Q\left(u-\sqrt{\frac{6r}{\left(\frac{E_b}{N_0}\right)^{-1}+\left(\frac{E_b}{N_I}\right)^{-1}\frac{1}{\rho}}}\right)du\right]\right\}$$

$$+Q\left((1+a)\sqrt{\frac{6r}{\left(\frac{E_b}{N_0}\right)^{-1}+\left(\frac{E_b}{N_I}\right)^{-1}\frac{1}{\rho}}}\right) \tag{5.22}$$

and $p_{s_{I_0}}$ is given by (5.21).

Now substituting (5.21) and (5.22) into

$$p_{s_I} = \rho p_{s_{I_I}} + (1-\rho) p_{s_{I_0}} \tag{5.23}$$

we obtain the overall probability of channel symbol error for the I-signal component. Now substituting (5.4) and (5.8) into

$$p_e = p_{e_{I_I}}(1+2p_{c_{I_I}}), \tag{5.24}$$

we obtain the overall probability of symbol erasure. Substituting (5.8) into

$$p_c = p_{c_{I_I}}{}^2, \tag{5.25}$$

we obtain the overall probability of correct symbol detection. Finally, substituting (5.23) into

$$p_s = p_{s_I}(2-p_{s_I}), \tag{5.26}$$

we obtain the overall probability of symbol error. The probability of block error is given by (2.29), the probability of symbol error is given by (2.30), and the probability of bit error is given by [2]

$$P_b = \left(\frac{1+m}{2m}\right)P_s. \tag{5.27}$$

Performance of the alternative waveform was evaluated for values of a between 0.1 and 0.6 and for a range of values of E_b/N_0, and the best overall performance is

obtained for $a = 0.4$. The performance of the alternative waveform in PNI with errors-and-erasures decoding when $a = 0.4$ and $E_b / N_0 = 10$ dB is shown is Figure 9.

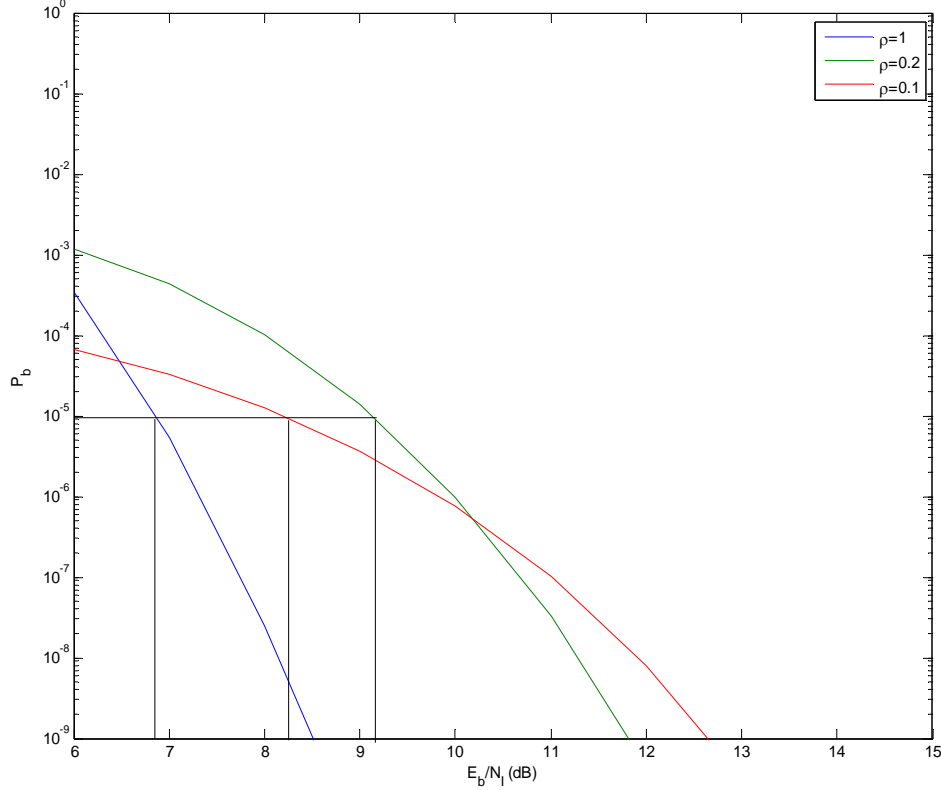

Figure 9.   Performance of complex 8-BOK with a (63, 37) RS code with errors-and-erasures decoding where a=0.4 and $E_b / N_0 = 10$ dB.

The E_b / N_I required for $P_b = 10^{-5}$ when $E_b / N_0 = 10$ dB and $a = 0.4$ are shown in Table 4. In this case, $\rho = 0.2$ degrades performance by an additional 2.2 dB as compared to $\rho = 1.0$, and $\rho = 0.1$ improves performance by an additional 0.9 dB as compared to $\rho = 0.2$. Comparing the results from Table 4 with the results from Table 3, we see that with errors-and-erasures decoding there is a slight improvement in performance of 0.2 dB when $\rho = 1.0$ and much more noticeable improvement of 1.6 dB when $\rho = 0.1$. In fact, errors-and-erasures decoding increases the value of ρ which maximize the E_b / N_I required to achieve $P_b = 10^{-5}$.

Table 4.   Performance of complex 8-BOK with a (63, 37) RS code for $P_b = 10^{-5}$ and errors-and-erasures decoding with a=0.4 and $E_b / N_0 = 10$ dB.

ρ	E_b / N_I
$\rho = 1$	6.9 dB
$\rho = 0.2$	9.1 dB
$\rho = 0.1$	8.2 dB

D.   CHAPTER SUMMARY

In this chapter, the performance of complex 8-BOK with a (63, 37) RS code and errors-and-erasures decoding was investigated for both AWGN alone and AWGN and PNI together. Next, the union bound on the probability of symbol error for *MBOK* with errors-and-erasures demodulation was derived. Comparing the results obtained in this chapter with those obtained in the previous chapter, we conclude that errors-and-erasures demodulation improves performance by about 1.6 dB.

In the next chapter, the performance of complex 8-BOK with a (63, 37) RS code is compared to that of TCM for both AWGN and PNI.

THIS PAGE INTENTIONALLY LEFT BLANK

VI. COMPARISON OF THE PERFORMANCE OF COMPLEX 8-BOK WITH A (63, 37) RS CODE TO THAT OF TCM IN AWGN AND PNI

In this chapter, the performance of complex 8-BOK with a (63, 37) RS code vs. the performance of TCM in AWGN is compared by analyzing the probability of bit error vs. E_b / N_0. A similar comparison is made when PNI is also present.

A. COMPARISON OF THE PERFORMANCE COMPLEX 8-BOK WITH A (63, 37) RS CODE VS THE PERFORMANCE OF TCM IN AWGN

As we see from Figure 4, for $P_b = 10^{-5}$ the alternative waveform requires $E_b / N_o = 5.5$ dB, while from Figure 10 $E_b / N_o = 5.3$ dB is required for TCM. Hence, the alternative waveform is 0.2 dB poorer than the TCM system. For all practical purposes, 0.2 dB is small enough that the two systems can be considered to be roughly comparable.
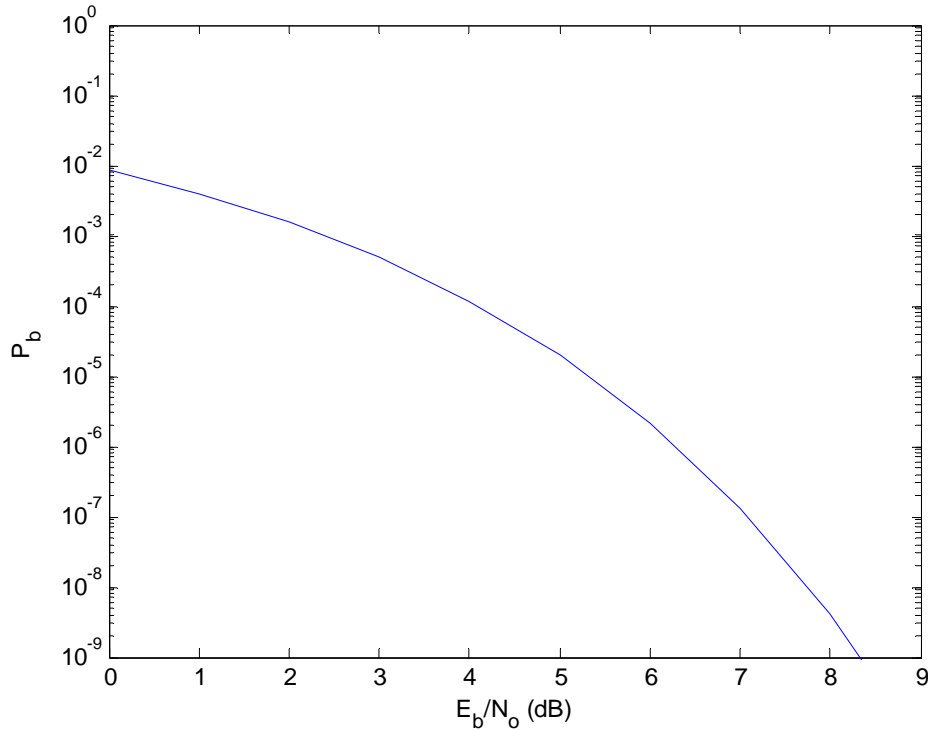

Figure 10.   TCM system performance with 8-PSK modulation and an $r = 2/3$ encoder with K=4 and natural mapping in AWGN (From: [3]).

B. COMPARISON OF THE PERFORMANCE COMPLEX 8-BOK WITH A (63, 37) RS CODE VS THE PERFORMANCE OF TCM IN PNI

In Figures 11 and 12, the performance of 8-PSK, $r=2/3$, TCM with $K=4$ and the performance of complex 8-BOK with a (63, 37) RS code, respectively, are plotted when PNI is present with $E_b/N_o = 7.8$ dB. The results for 8-PSK, $r=2/3$, TCM with $K=4$ and PNI with $E_b/N_o = 7.8$ dB are summarized in Table 5, and the results for complex 8-BOK with a (63, 37) RS code and PNI with $E_b/N_o = 7.8$ dB are summarized in Table 6. As can be seen from Table 6, $\rho = 0.2$ degrades the performance of the alternative waveform by an additional 1.9 dB, while from Table 5 we see that the maximum degradation due to PNI is 2.7 dB when $\rho = 0.1$, an increase of 0.8 dB in relative degradation. From Figure 11, we see that $\rho = 0.2$ does not result in the maximum performance degradation for TCM as it does for the alternative waveform. Finally, we note that when $\rho = 0.1$, the alternative waveform outperforms the TCM waveform by 1.1 dB.
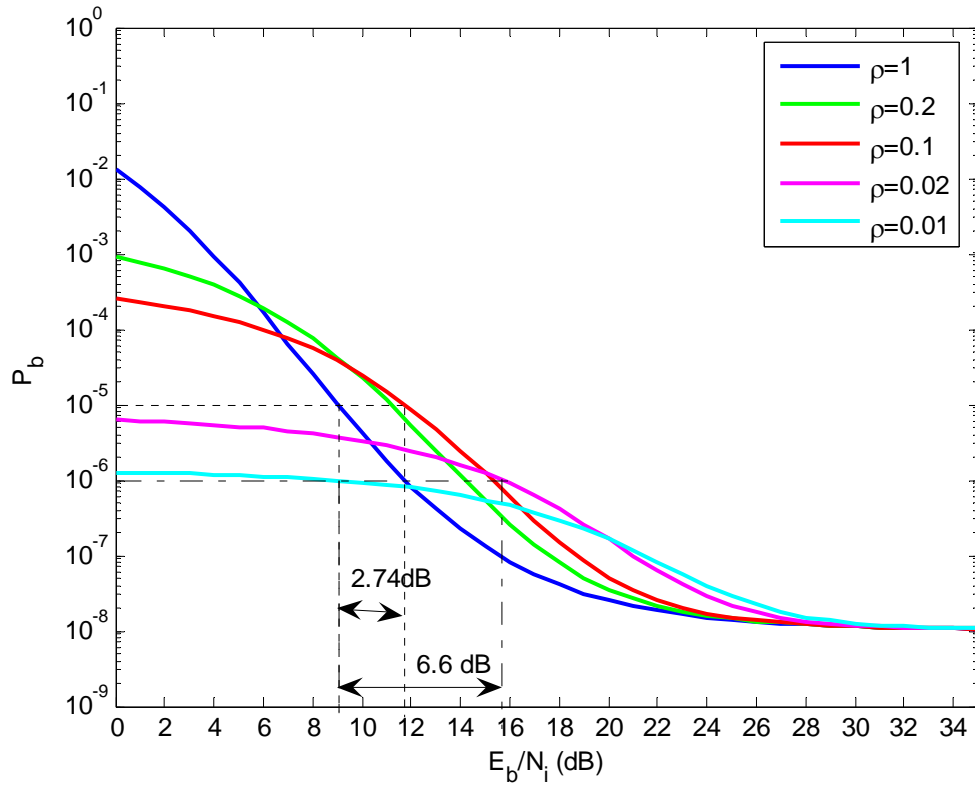
Figure 11.   Performance of 8-PSK, *r*=2/3, TCM with *K*=4 and PNI with E_b / N_o = 7.8 dB (From: [3]).

Table 5.   Performance of 8-PSK, *r*=2/3, TCM with *K*=4 for $P_b = 10^{-5}$ in PNI when E_b / N_o = 7.8 dB

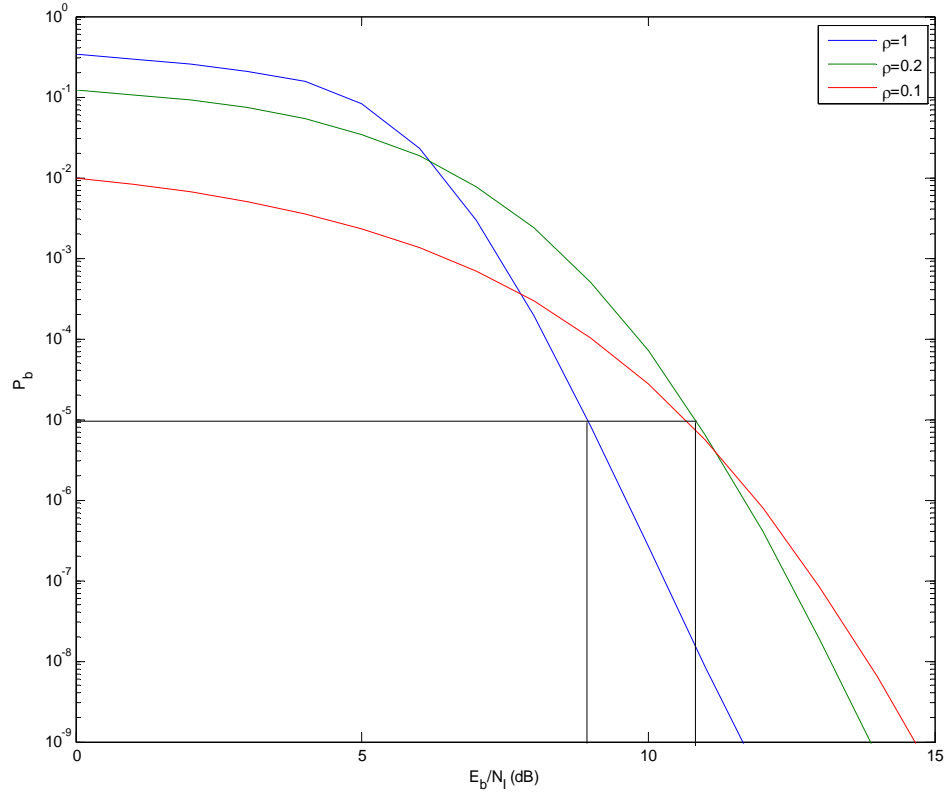| ρ	E_b / N_I
$\rho = 1$	9.0 dB
$\rho = 0.1$	11.7 dB

Figure 12.   Performance of complex 8-BOK with a (63, 37) RS code and PNI with
$E_b / N_o = 7.8$ dB.

Table 6.   Performance of complex8-BOK with a (63, 37) RS code for $P_b = 10^{-5}$ in PNI
when $E_b / N_o = 7.8$ dB.

ρ	E_b / N_I
$\rho = 1$	8.9 dB
$\rho = 0.2$	10.8 dB
$\rho = 0.1$	10.6 dB

C.   CHAPTER SUMMARY

In this chapter, the performance of complex 8-BOK with a (63, 37) RS code was compared with the performance of TCM in AWGN and PNI. When only AWGN is present, the two systems are roughly comparable, but when PNI is also present, the alternative waveform is 1.1 dB better.

In the next chapter, the conclusions and recommendations are presented.

THIS PAGE INTENTIONALLY LEFT BLANK

VII.   CONCLUSIONS AND RECOMMENDATIONS

A.   CONCLUSIONS

The performance of a communication system having almost the same spectral efficiency as a trellis coded modulation (TCM) system with r = 2/3 convolutional encoding and 8-*ary* phase-shift keying (8-PSK) modulation was investigated. TCM is a common solution to the problem of adding forward error correction (FEC) coding without an attendant increase in channel bandwidth. The primary drawback to TCM is that the achievable coding gain is limited by the maximum practical number of states in the convolutional encoder. The alternative system considered uses (63, 37) Reed-Solomon (RS) encoding. The six-bit symbols at the output of the Reed-Solomon encoder undergo serial-to-parallel conversion to two three-bit symbols, which are then independently transmitted on the in-phase (I) and quadrature (Q) component of the carrier using 8-*ary* biorthogonal keying (8-BOK). This system has a null-to-null bandwidth of $0.993R_b$, which is 0.7% smaller than TCM with r = 2/3 convolutional encoding and 8-PSK modulation. The effect of both AWGN and PNI on the alternative waveform are investigated and compared to the effect of the same type of noise on a TCM signal.

In AWGN, the alternative system requires $E_b / N_o = 5.5$ dB to achieve $P_b = 10^{-5}$ as compared to 5.3 dB for TCM. When PNI is also present, as E_b / N_0 increases, the relative degradation due to PNI increases. This seemingly counterintuitive result can be understood by noting that, while relative performance in PNI is degraded when E_b / N_0 increases, absolute performance is improved. When $E_b / N_0 = 5.6$ dB, $E_b / N_I = 17.8$ dB is required for $P_b = 10^{-5}$, while when $E_b / N_0 = 6.1$ dB, only 0.5 dB more, $E_b / N_I = 14.2$ dB is required for $P_b = 10^{-5}$. This trend continues as E_b / N_0 increases, as can be seen from the results obtained when $E_b / N_0 = 10$ dB, where the maximum degradation due to PNI is 2.8 dB, but $E_b / N_I < 10$ dB is required for $P_b = 10^{-5}$. For realistic values of

E_b / N_0, the performance of a TCM system with a comparable spectral efficiency when PNI is present is inferior to the performance of the alternative waveform by about 1.1 dB in terms of E_b / N_I.

The performance of complex 8-BOK with a (63, 37) RS code and errors-and-erasures decoding was also investigated. The benefit of errors-and-erasures decoding when only AWGN is present is negligible, but when PNI is also present, errors-and-erasures decoding improves performance by about 1.6 dB.

B.   RECOMMENDATIONS

We have examined an alternative to TCM for waveforms transmitted over a channel with PNI. The effect of transmitting the alternative waveform over a flat, slowly fading, Nakagami channel should be investigated.

Presumably, the advantage of the alternative system over TCM when PNI is present would be diminished if the TCM encoder had more than sixteen states. In order to investigate this, the performance of the TCM system would have to be obtained by simulation rather than analysis since the analysis of TCM with more than a 16-state encoder is extremely difficult when PNI is present. Nevertheless, it seems reasonable to conclude that the performance of the alternative system examined in this thesis would be comparable.

LIST OF REFERENCES

[1]   Daniel J. Costello and Shu Lin, Error Control Coding: *Fundamental and Applications*, 2nd edition, Prentice-Hall, Upper Saddle River, NJ, 2004.

[2]   Clark Robertson, Notes for EC4580 (Error Correction Coding), Naval Postgraduate School, Monterey, CA, 2007 (unpublished).

[3]   Ioannis Katzourakis, *Performance Analysis of Variable Data Rate TCM Waveform Transmitted Over a Channel With AWGN and Pulse Noise Interference* Master's Thesis, Naval Postgraduate School, Monterey, CA, 2007.

[4]   Clark Robertson, Notes for EC4550 (Digital Communications), Naval Postgraduate School, Monterey, CA, 2007 (unpublished).

[5]   B. Sklar, *Digital Communications: Fundamental and Applications*, 2nd edition, Prentice-Hall, Upper Saddle River, NJ, 2001.

THIS PAGE INTENTIONALLY LEFT BLANK

INITIAL DISTRIBUTION LIST

1.   Defense Technical Information Center
        Ft. Belvoir, Virginia

2.   Dudley Knox Library
        Naval Postgraduate School
        Monterey, California

3.   Chairman, Code EC
        Department of Electrical and Computer Engineering
        Monterey, California

4.   Chairman, Code IS
        Department of Information Sciences
        Monterey, California

5.   Professor R. Clark Robertson, Code EC/Rc
        Department of Electrical and Computer Engineering
        Monterey, California

6.   Professor Tri Ha, Code EC/Ha
        Department of Electrical and Computer Engineering
        Monterey, California

7.   Mario Marques
        Lisbon, Portugal